frontiers in Materials

ORIGINAL RESEARCH
published: 03 January 2022
doi: 10.3389/fmats.2021.803106

Property Evaluation of Cement-Stabilized Macadam Modified *via* Phosphorus Slag Materials

Guoping Qian[1,2], *Wei Liu*[1], *Xiangbing Gong*[1]*, *Xi Li*[1] and *Yalong Zhang*[1]

[1]School of Traffic and Transportation Engineering, Changsha University of Science and Technology, Changsha, China, [2]National Engineering Laboratory for Highway Maintenance Technology, Changsha University of Science and Technology, Changsha, China

Phosphorus slag, known as the waste product of the phosphate ore industry, is causing critical environmental issues due to its direct exposure to natural spaces. In this article, a partial replacement of the natural fine aggregate ordinarily used in cement-stabilized macadam (CSM) base by phosphorus slag was explored to be an effective solution for phosphorus slag waste. CSM specimens were fabricated by adding various dosages of phosphorus slag particle and fine powder, whereas the optimum moisture content and maximum dry density were analyzed through compaction tests. Compressive strength, bending tensile strength, fatigue life span, dry shrinkage, and temperature shrinkage performance at different curing durations were investigated to evaluate the properties of modified macadam. Results show that phosphorus slag reduced the early compressive strength of CSM to a small extent, but the compressive strength finally increased at 90 days' curing. The modified slag particles and slag fine powder exhibited different behaviors to repeated loading, moisture loss, and temperature difference. Finally, according to the strength change, fatigue performance comparison, and shrinkage strain caused by the incorporation of phosphorous slag materials into the CSM, it was verified that 25% of the particles to 40% of the fine powder is the best replacement ratio.

Keywords: semirigid base, cement-stabilized macadam, phosphorus slag aggregate, strength, crack resistance, fatigue

OPEN ACCESS

Edited by:
Hui Yao,
Beijing University of Technology, China

Reviewed by:
Yue Xiao,
Wuhan University of Technology, China
Tao Ma,
Southeast University, China

***Correspondence:**
Xiangbing Gong
xbgong@csust.edu.cn

Specialty section:
This article was submitted to Structural Materials, a section of the journal Frontiers in Materials

Received: *27 October 2021*
Accepted: *01 December 2021*
Published: *03 January 2022*

Citation:
Qian G, Liu W, Gong X, Li X and Zhang Y (2022) Property Evaluation of Cement-Stabilized Macadam Modified via Phosphorus Slag Materials. Front. Mater. 8:803106. doi: 10.3389/fmats.2021.803106

INTRODUCTION

With the rapid development of the yellow phosphorous industry, the current yellow phosphorous production volume is increasing day by day. From 2017 to 2020, China's output exceeded 1 million tons. At the same time, the output of phosphorous slag is large, causing serious environmental pollution (Zhang and Cao, 2012). Therefore, the treatment of phosphorous slag has become a problem that needs to be solved, which has also prompted research on some new topics in the development of green transportation (Sun et al., 2020a; Bujang et al., 2018; Nanjegowda and Biligiri, 2020) and turning waste into resources. In recent years, many researchers have processed steel slag (Guo et al., 2018; Tang et al., 2020) and blast furnace slag (Shi et al., 2021) to reduce a large amount of environmental pollution. Concurrently, researchers have also considered the use of phosphorous slag from many aspects. For example, researchers have used waste phosphorous slag in cement concrete, and the addition of phosphorous slag materials has improved the performance of cement concrete

(Hu, 2017; Pang et al., 2020; Li et al., 2015). European researchers used three different types of industrial wastes: cement kiln dust, granular blast furnace slag, and marble sludge, to make artificial bones and prove sustainable production (Colangelo and Cioffi, 2013). Researchers in the United States have analyzed the composition of various slags and put forward the use cases for various slags (Piatak et al., 2015). Chinese researchers have used phosphorous slag as a filler in hot-mix asphalt mixtures and conducted a large number of indoor tests, showing that phosphorous slag is feasible as a road pavement material (Qian et al., 2013).

Therefore, the research done by researchers for reference shows that the phosphorous slag material can be fully utilized in the pavement base layer, and the economic value it brings is quite considerable. Among them, the semirigid cement-stabilized macadam (CSM) base is the most widely used base course in China. CSM base has excellent properties, such as compressive strength, rigidity, fatigue resistance, bending tensile strength, and strong load spreading ability, so it is widely used in highway bases or sub-bases (Li et al., 2021; Du et al., 2019; Lv et al., 2019a; Lv et al., 2021b). However, this material still has some defects as a base: (1) the shrinkage and cracking of the CSM base can cause different reflective cracks in the asphalt pavement (Farhan et al., 2018; You et al., 2020); (2) the CSM has poor water seepage performance; (3) after the CSM base is damaged, it cannot be repaired; (4) the CSM base has excellent integrity, but as the use time increases, the strength and modulus of the material will gradually decay due to fatigue factors under repeated loads. This, in turn, leads to structural damage to the substratum and ultimately to the destruction of the board structure (Lv et al., 2021). Among them, early reflective cracks are the main defect (Gao, 2019; Li et al., 2019) and can be remedied by using a slow-setting microexpansion cement to replace the ordinary cement, effectively compensating for the shrinkage of ordinary cement, thereby improving the volume stability in terms of shrinkage and reducing the shrinkage cracks of the CSM base layer. Sun et al. (2020b) through research found that rubber particles made from waste tires are added to the CSM according to different particle sizes and ratios. Through the dry shrinkage test, it is found that the addition of rubber powder can significantly improve the antivolume shrinkage capacity of the CSM, thereby preventing the formation and expansion of initial cracks. Yang et al. (2020) and Jing et al. (2021) have shown through research that adding a geogrid at the bottom of a semirigid base can delay the propagation of reflective cracks on the asphalt pavement.

As the semirigid base has several problems such as cracking, poor water permeability, and failure to repair after damage, it is necessary to study and analyze the above problems of the semirigid base. The method of applying semirigid base treatment is done by first optimizing the design from the structure itself and then selecting and replacing the material type (Ma et al., 2015; Zheng et al., 2019) and finally checking if material modification is feasible (Xue and Jiang, 2017). Despite all this, material replacement is still the most convenient and cost-saving effective way to solve the performance defects of semirigid bases. The particle size distribution of phosphorus slag particles is similar to the fine aggregate particle size distribution in the CSM mixture. In addition, the phosphorous slag material itself is also a potential hydraulically active material with high latent strength (Wang et al., 2021), good sulfate resistance, anticorrosion ability (Wang et al., 2019; Allahverdi et al., 2017), strong impermeability, and durability (Vafaei and Allahverdi, 2019). It can also reduce the heat of hydration in the mixture and possesses high flexural strength and good abrasion performance (Qian et al., 2019). Therefore, the replacement of the material in the semirigid base with phosphorous slag material has become one of the most sought-after research paths.

In summary, this article discusses the feasibility of applying phosphorous slag materials to the CSM base and identifying the optimal proportion of phosphorous slag materials through laboratory experiments. In the experiment, two ways to add phosphorous slag material to the CSM mixture are explored: by using phosphorous slag particles to replace part of the macadam in the CSM mixture and by replacing part of the cement in the CSM mixture with finely ground phosphorous slag fine powder. The 7-day unconfined compressive strength test on the CSM mixture with phosphorous slag material is used to determine whether the mixture ratio design is reasonable. Through the analysis of the influence of phosphorus slag materials on the strength, fatigue performance, and crack resistance of CSM mixtures, the comprehensive evaluation and analysis of the performance of CSM mixtures with phosphorous slag materials in different proportions are studied.

MATERIALS AND METHODS

Fundamental Properties of Raw Materials

Phosphorus slag particle is well-known to be a porous material with complicated shapes. From an appearance point of view, the phosphorous slag particles are either off-white or light yellow, and some have a porous and glassy luster-like structure alongside an uneven particle shape. Existing studies have shown that phosphorus slag particles are irregular in appearance under electron microscope scanning. There are many uneven pores on the surface of phosphorus slag particles, and the pore diameters of these pores are in the order of tens to hundreds of microns. Its physical properties are similar to the macadam used in a semigrid base. The apparent relative density of phosphorus slag particles is 2.60 g/cm^3. After placing 100 g of phosphorus slag in the room for 15 days, the weight of the phosphorus increased to 100.2 g, so the storage stability in the air is stable. The gradation of slag particles is shown in **Figure 1**, and the maximum particle size is 4.75 mm.

Phosphorus slag fine powder is formed by grinding phosphorous slag particles. According to the fundamental tests, its specific surface area is 380 m^2/kg, and the percentage of material larger than 0.075 mm in the phosphorous slag fine powder measured by the water washing method is only 1.8%. Other physical property tests were conducted by following the experimental specification named Highway Engineering Aggregate Test Regulations (JTG E42-2005-2005, 2005) used in China (2005); results are listed in **Table 1**.

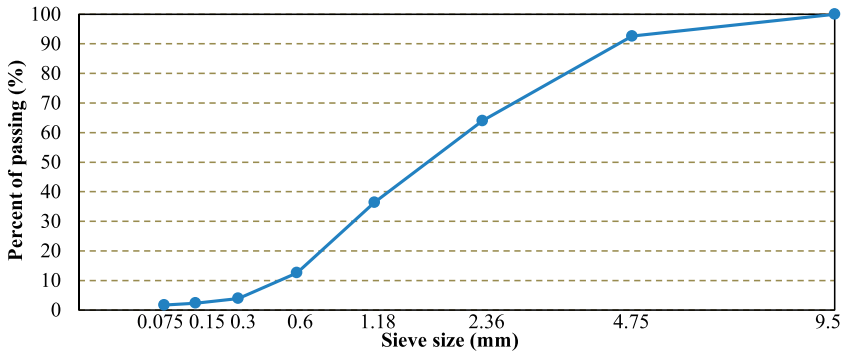

FIGURE 1 | Gradation of phosphorus slag particles.

TABLE 1 | Physical properties of phosphorus slag fine powder.

Pilot projects		Technical limits	Testing value	Specification code
Apparent density (g/cm^3)		≥2.50	2.92	T0352-2000
Moisture content (%)		≤1	0.2	T0103-2000
Particle passing (%)	<0.6 mm	100	100	T0351-2000
	<0.15 mm	90–100	100	T0351-2000
	<0.075 mm	75–100	98.2	T0351-2000
Hydrophilic coefficient		<1	0.6	T0353-2000
Alkalinity or acidity		Acidity <7 < alkalinity	9.9	Testing paper

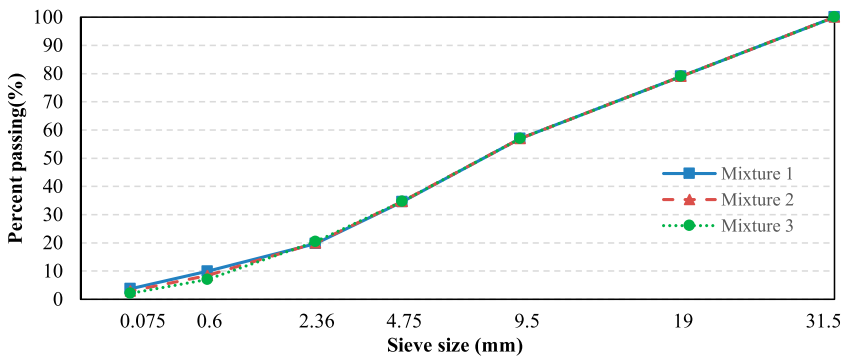

FIGURE 2 | Gradation of CSM with different dosages of phosphorus slag particles.

Ordinary Portland cement is used as the cement, and the compressive strength of the cement mortar after 28 days of curing should theoretically be bigger than 42.5 MPa. In the CSM mixture, the Portland cement dosage is 4%. Except for phosphorus slag, aggregates are limestones obtained from a local stockyard in Changsha. In this study, the Portland cement and limestone aggregate meet the limits required by the semigrid base specification.

Experiment Methods

Two types of replacement methods were applied in modified macadam. The first is to replace a part of the aggregate with phosphorus slag particles, and the second is to replace a part of the cement with phosphorus slag fine powder. The phosphorous slag particles are mixed at different replacement rates. Among them, it can be seen from **Figure 1** that the particle size distribution of the phosphorus slag particles and the 0- to 5-mm fine aggregate are close. Therefore, by sieving the phosphorus slag particles and replacing some of the 0- to 5-mm fine aggregate with the phosphorus slag particles to form a composite aggregate, three comparative experimental groups were obtained, as shown in **Figure 2**. The maximum dry density and optimum moisture content of three mixtures were obtained through the compaction test. Phosphorus slag fine powder is used to replace cement in the macadam. The total dosage of cement and phosphorus slag fine powder is kept at a constant of 4%.

Following the requirements of the "Test Methods of Materials Stabilizing with Inorganic Binders for Highway Engineering" (JTG E51-2009-2009, 2009), the compressive strength test, bending tensile strength test, fatigue test, and shrinkage test were listed to evaluate the performance of the phosphorous slag material–modified macadam.

Compressive Strength Test

The measurement of unconfined compressive strength requires a cylinder specimen with a size of φ150 mm × h150 mm. Each testing group prepared nine specimens at the same curing duration. The mass (M_{real}) of a specimen was calculated based on **Eq. 1**, and all sample preparation procedure follows the mass determination rule.

$$\boldsymbol{M_{real} = V \times P_{max} \times \left(1 + W_{opt}\right) \times r \times (1 + \alpha)} \quad (1)$$

where V is the volume of a cylinder test mold, P_{max} is the maximum dry density of the mixture, W_{opt} is the best moisture content of the mixture, r is equal to 98%, and α refers to a compensation factor with a value of 1% because of mass loss while loading the materials.

Following the test method specification, specimens were formed by static pressure, and then samples were transported to the curing room after sealing. The temperature in the curing room is 20°C ± 2°C, and the humidity must be greater than 95%. For the unconfined compressive strength test, the specimen is taken out on the last curing day and immersed into a water tank at 20°C ± 2°C; the top surface of the specimen should be covered by water with a thickness of 2.5 cm. After soaking for 24 h and wiping off the surface moisture, samples were compressed at a rate of 1 mm/min, and compressive strength can finally be obtained based on the maximum loading force.

Bending Tensile Strength Test

A beam with a size of 100 × 100 × 400 mm is selected for the bending test. The MTS Landmark 370.10 multifunctional material testing system, made in the United States, was used to conduct bending tensile testing. The test was carried out using the three-point bending method, with a loading rate of 50 mm/min.

Through the data collection and processing, the maximum load is obtained. The bending tensile strength can be calculated according to **Eq. 2**.

$$\boldsymbol{f = \frac{FL}{bh^2}} \quad (2)$$

where F refers to the failure load, L is the distance between the two support points, and b and h are the width and height of the test piece, respectively. According to the measurement and the size of the test piece, it is found that L is 300 mm, and b and h are 100 mm.

To ensure the reliability of the test data, a total of five specimens were measured in this test. The arithmetic means to value and error were calculated from the obtained data.

Fatigue Test

The fatigue test adopts a repeated stress control mode, while the testing beam was prepared with a size of 100 × 100 × 400 mm. The fatigue test adopts a three-point bending test undergoing Haversine wave dynamic periodic compressive stress load mode. The load frequency is 10 Hz, whereas the maximum load and minimum load are listed in **Eq. 3**.

$$\boldsymbol{P_{max} = \alpha \times F;\ P_{min} = P_{max} \times \beta} \quad (3)$$

where α is the stress ratio within the value range 0.5 to 0.8, F is the average bending tensile strength of each mixture, and β is the characteristic factor of the load cycle; β is equal to 0.1.

To reduce the test deviation, the testing beam should be pre-pressed with a force of 1 KN for 2 min before the fatigue test, which will reduce the bad contact between the specimen and the mold.

Shrinkage Test

The size of the specimen used in the shrinkage test is 100 × 100 × 400 mm, and the curing duration is 7 days. To ensure the accuracy of the test data, three test pieces were done to get an average value. Accounting for the dry shrinkage, both ends of the test piece were properly polished with sandpaper, and then glass sheets were pasted on the surface. To reduce the friction, a certain number of steel balls were placed on the glass. As the shrinkage strain mainly occurs in the first few days, the number of readings should be increased at the beginning of the test and should be recorded every 6 hours for the first 2 days, twice a day from the third to the fourth day, every 2 days after 4 days, and every 7 days after 14 days. The weighting electronic balance used for the test has a sensitivity of 1 g, a maximum range of 15 kg, and a vernier caliper graduation of 0.01 mm. This article adopts the strain gauge method to measure the temperature shrinkage strain of CSM. After 7 days of curing, the specimens were placed in an oven at 105°C ± 0.5°C lasting for 10 h to eliminate the dry shrinkage strain caused by the evaporation of water. The temperature compensation sheets were made out of inorganic silicate materials, and the strain gauges are foil-type resistance strain gauges with a resistance of 120 Ω and a gauge length of 80 mm. The test temperature is gradually reduced from 50°C to 0°C at intervals of 10°C. Samples should be placed in the oven for 3 h when the temperature drops to the testing temperature.

ANALYSIS AND DISCUSSION

Compaction Characterization

In **Figure 2**, mixtures 1, 2, and 3 refer to the ratio of phosphorous slag particles in place of stone aggregate at 0%, 25%, and 50%, respectively. Through the compaction test, the obtained optimum moisture content and the maximum dry density are shown in **Figure 3**.

The compaction results show that the phosphorous slag particle decreases the maximum dry density and increases the optimum moisture content. Because phosphorous slag particles have a porous structure, their apparent relative density is lower, and water absorption is greater. After a large number of repeated tests, it can be concluded that the replacement of cement by phosphorous slag fine powder will not significantly affect the maximum dry density and optimal moisture content of the

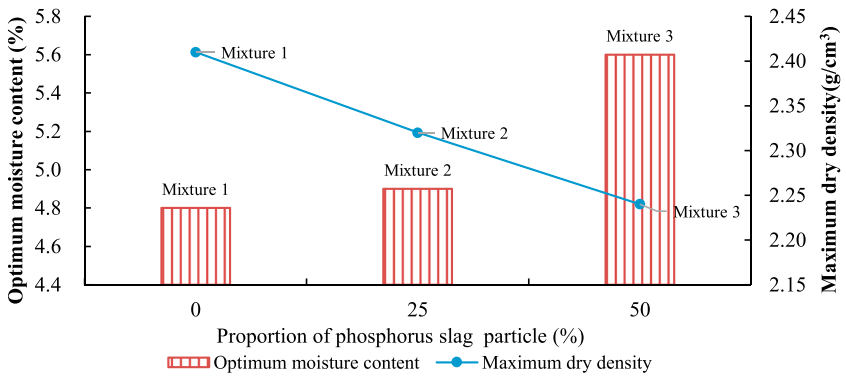

FIGURE 3 | The optimum moisture content and maximum dry density of the CSM mixtures.

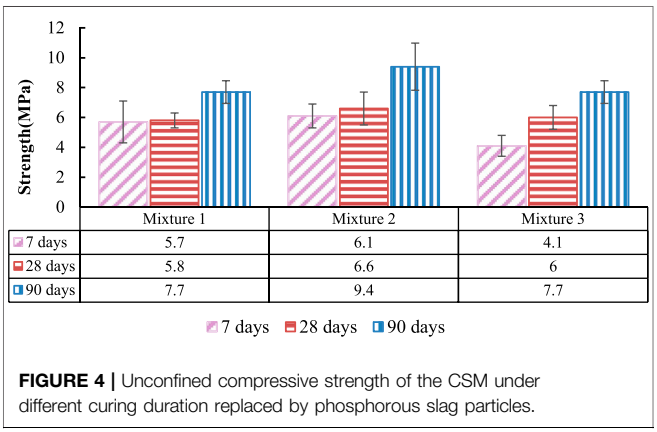

	Mixture 1	Mixture 2	Mixture 3
7 days	5.7	6.1	4.1
28 days	5.8	6.6	6
90 days	7.7	9.4	7.7

FIGURE 4 | Unconfined compressive strength of the CSM under different curing duration replaced by phosphorous slag particles.

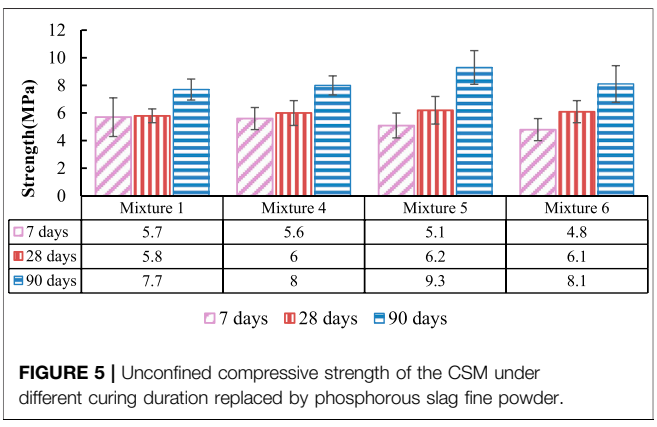

	Mixture 1	Mixture 4	Mixture 5	Mixture 6
7 days	5.7	5.6	5.1	4.8
28 days	5.8	6	6.2	6.1
90 days	7.7	8	9.3	8.1

FIGURE 5 | Unconfined compressive strength of the CSM under different curing duration replaced by phosphorous slag fine powder.

macadam. Therefore, the mixtures 4, 5, and 6 in this section refer to the proportion of phosphorous slag fine powder to replace Portland cement at 20%, 40%, and 60%, and the first grade of the mixture is used.

Compressive Strength

Figure 4 shows the strength of the macadam at 7, 28, and 90 days after being modified by phosphorous slag particles. **Figure 5** exhibits the strength of the macadam at 7, 28, and 90 days after being modified by phosphorous slag fine powder.

Phosphorous slag particles and phosphorous slag fine powder CSM mixtures decreased in strength at 7 days' curing, as shown in **Figures 4**, **5**. Mixtures 2 and 5 presented the highest compressive strength at 90 days' curing in their experimental group. In contrast with mixture 1, mixture 2 increased by 1.7 MPa, and mixture 5 increased by 1.6 MPa. Although the early strength of CSM mixtures mixed with phosphorus slag materials will be lower, the strength eventually becomes greater than that of mixture 1 as the curing continues. Results show that strength increases faster in the early stage and gradually becomes slower and slower. The early strength of the CSM mixed with phosphorous slag material decreases because the slurry formed by the phosphorous slag material and water is generally not hydraulic. The strength of the modified macadam at the later stages improved because of the calcium hydroxide produced by the hydration process of cement. Calcium hydroxide is known to be an activator that causes the phosphorus slag materials to rapidly complete the hydration and cementing reaction. Chemical components of the phosphorous slag are active materials; after the secondary reaction, it will increase the strength of the CSM and optimize the inner structure and pore size distribution.

Bending Tensile Strength

From the results of the compressive testing results, it is found that mixtures 2 and 5 possessed the largest bending strength in **Figure 6** shows that compared with mixture 1 without adding any phosphorous slag materials, the bending tensile strength of mixtures 2 and 5 increased by 0.572 and 0.794 MPa. As mentioned previously, active silica and aluminum oxide in phosphorous slag materials react with calcium hydroxide in cement to form calcium silicate and calcium aluminate, which causes the bending tensile strength of phosphorous slag material–modified macadam to increase significantly. Compared with the compressive strength at 90 days, phosphorous slag fine powder enhances the bending tensile strength better than phosphorous slag particles. Phosphorous

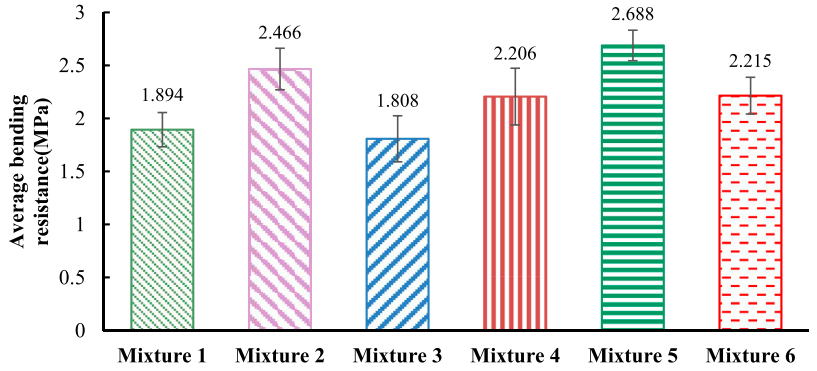

FIGURE 6 | Bending tensile strength of the CSM at 90 days' curing.

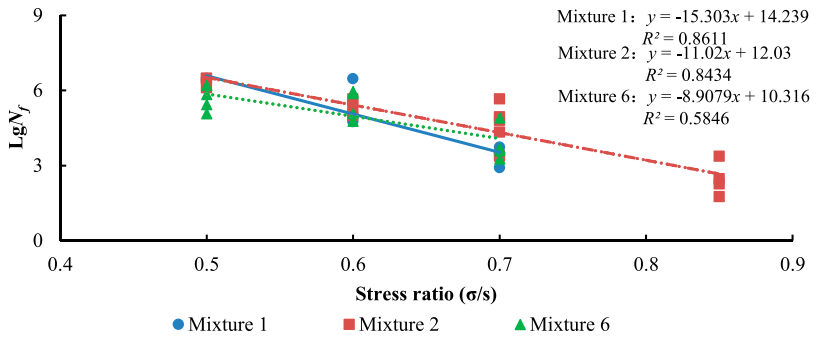

FIGURE 7 | *S-N* curves of different CSM mixtures.

slag fine powder is proven to be an effective replacement for Portland cement concerning the strength of macadam.

Resistance to Fatigue

In the semirigid asphalt pavement structure, the base of the CSM is the predominant layer to bear the repeating load. Therefore, the fatigue performance of the base material is an important factor when considering the material and structural design of asphalt pavement. The *S-N* curve, based on the stress controlling model, is commonly used to represent fatigue life, where *S* is the stress ratio and *N* is the repeating load number, while the modulus decreases to 50% of the origin modulus. After 90 days' curing, the *S-N* curves and linear fitting equation at the semilog coordinate of mixtures 1, 2, and 6 are shown in **Figure 7**.

The slope of the *S-N* curve of the original CSM is larger than the phosphorous slag material–modified macadam, which shows that a small change in stress level has a great impact on the fatigue life of virgin CSM. Accounting for the phosphorous slag materials, phosphorous slag fine powder (mixture 6) exhibited a weakening effect on the fatigue life at a small stress ratio level compared with the other two mixtures (mixtures 1 and 2). Nonetheless, fine powder enhances the resistance to fatigue as the stress ratio grows to 0.7. Phosphorous slag particles are proven to be less sensitive to stress levels because the largest N_f undergoes various stress ratios. Therefore, phosphorous slag materials might increase the fatigue life span of the base layer of asphalt pavement, especially when subjected to heavy-duty traffic.

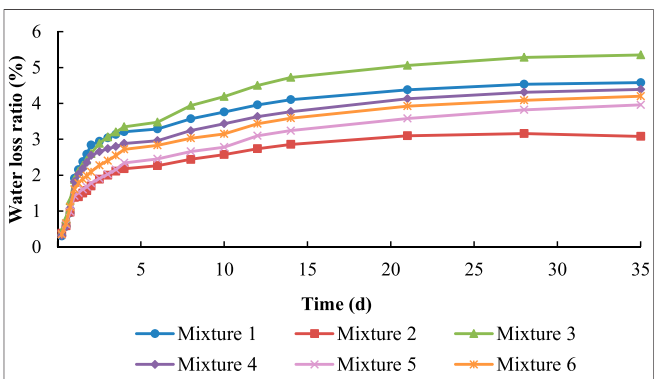

FIGURE 8 | Water loss ratio of different experimental groups.

Shrinkage

Drying shrinkage is a critical factor in the forming of cracks on the semirigid base layer. Therefore, increased resistance to drying shrinkage is generally associated with the increased life span of asphalt pavement using CSM. Drying shrinkage is predominantly caused by the decrease of the moisture content of the mixture

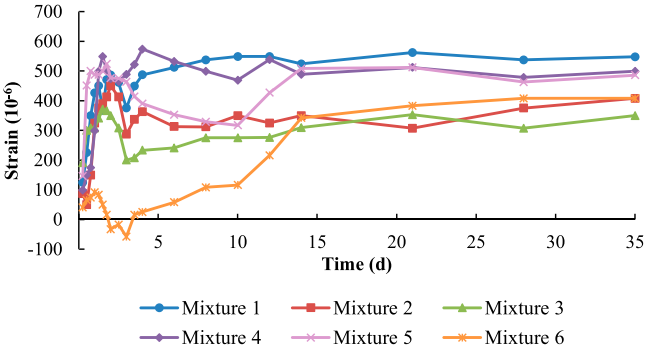

FIGURE 9 | Drying shrinkage strain of different experimental groups.

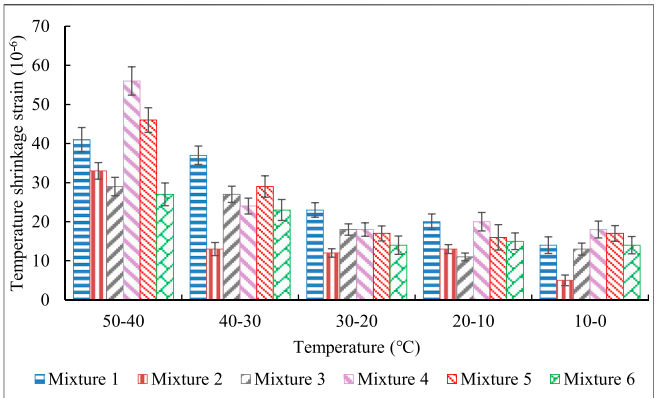

FIGURE 10 | Temperature shrinkage strain of different experimental groups.

through processes such as capillary tension, adsorption of water and intermolecular forces, carbonization, and dehydration. Water loss ratio and shrinkage strain were investigated to present the drying shrinkage of various testing groups, with results changing as the curing duration increases, as shown in **Figures 8**, **9**.

Phosphorous slag particle and phosphorous slag fine powder proved to be effective modifications to increase the resistance to drying shrinkage, as shown in **Figures 8**, **9**. The water loss ratio could laterally reflect the changing trend of the drying shrinkage strain of the CSM. Except for mixtures 3 and 6, the less the water loss implies the smaller the drying shrinkage. Phosphorous slag fine powder decreases the water loss ratio due to its strong water absorption compared with phosphorous slag particles. Water loss ratio shows stable varication other than drying shrinkage strain, especially during the first 5 days of the curing period. The water loss ratio trend could be easily distinguished at the beginning of the dry shrinkage.

However, shrinkage caused by drying presents complicated fluctuations, especially during the early drying period. The drying shrinkage ratio of phosphorous slag particle–modified macadam changes rapidly after 5°days of curing. Compared with the original CSM, the replacement of phosphorus slag particles helps to reduce the drying shrinkage strain, thereby achieving long-term performance. Apart from the material effect, fine gradation of mixture 1 leads to less space for volume shrinkage. Moreover, phosphorous slag particle content is less fine aggregate with a size less than 0.6°mm, which generates coarse gradation of the macadam in mixtures 2 and 3 and decreases the dry shrinkage strain to the largest gap.

Phosphorous slag fine powder is proven to be less sensitive to dry shrinkage than cement-stabilized materials, because of the smaller dry shrinkage strain found in testing groups modified by phosphorous slag fine powder. The retardation of the phosphorous slag fine powder mentioned previously provides a filler and water absorption function to avoid drying shrinkage volume. Phosphorous slag components reacted effectively with the calcium hydroxide to form a C-S-H cementitious material, which decreases the thickness of the water film around the aggregate. The interface transition zone could be improved by using phosphorous slag fine powder, which will cause the bonding force between the aggregate and the slurry to be enhanced and microcracks in the interface transition zone to be reduced.

Temperature shrinkage is another crack-related factor in the degradation of the pavement performance; the main reasons for temperature shrinkage are associated with solid-phase shrinkage and liquid phase contraction. From 50°C to 0°C, the temperature shrinkage strain of different experimental groups is shown in **Figure 10**. Phosphorous slag particle presents the most effective improvement of resistance to temperature shrinkage, especially in the 40°C–30°C zone of mixture 2. Furthermore, mixture 2 exhibits the smallest total temperature shrinkage strain when the temperature drops from 50°C to 0°C. It is well-known that fine powder results in a large temperature shrinkage strain than a coarse particle. It can be seen that the particle size of the phosphorous slag particles is concentrated in the range of 0.6 to 4.75°mm, so its powder content and clay content are less than those of the macadam, so the temperature shrinkage volume is smaller. Macadam modified with phosphorous slag fine powder exhibits similar behavior with the original CSM, accounting for the trend and total temperature shrinkage strain. Therefore, phosphorous slag fine powder is almost as sensitive as Portland cement to temperature shrinkage due to the particle size similarity.

CONCLUSION

Phosphorous slag, also well-known to be the by-product of mineral smelting, also causes environmental pollution when directly exposed to natural lands. Phosphorous slag particles and fine powder are suitable to act as the replacement of aggregate and cement of CSM used as the semirigid base of asphalt pavement. This study adopts compaction, strength, fatigue, and shrinkage testing to investigate the effect of phosphorous slag on the performance of CSM. The main conclusions are as follows:

Phosphorous slag particles affect the optimum moisture content and maximum dry density significantly when compared with phosphorous slag fine powder. The

compaction characteristics become complex as the replacement ratio of phosphorous slag particles increases; 25% particle and 40% powder ratios are found to be the optimum replacement ratio, due to their mixtures possessing the largest compressive strength and bending tensile strength. Phosphorous slag materials are effective modifications to improve fatigue resistance when undergoing heavy-duty traffic.

Accounting for the dry and temperature shrinkage, the gradation of phosphorous slag particles is proven to be a predominant factor. Phosphorous slag particles generate a coarser gradation compared with the original macadam because of its aggregate passing characteristic, which generates more voids and provides more space to allow volume variation due to shrinkage. Thus, the gradation of fine aggregates needs to be considered more in the shrinkage of base materials.

Active silica oxide and aluminum oxide found in phosphorous slag materials reacted with calcium hydroxide, known as the hydration product of Portland cement. The interface transit zone of cement and aggregate could be enhanced via this secondary reaction. It can be concluded that this is the reason that phosphorous slag fine powder increases the compressive strength, especially at 90°days' curing. Water absorption and filler function caused by the secondary reaction prevent the dry shrinkage issue found in phosphorous slag fine powder–modified macadam.

Future Work

To investigate the modification mechanism of phosphorous slag particles and fine powder, this study applies the single-doped method to conduct the experiments. Future work involves plans to design a compound modification testing procedure, which aims to achieve a high-performance macadam and high usage of waste phosphorous slag materials.

DATA AVAILABILITY STATEMENT

The original contributions presented in the study are included in the article/Supplementary Material; further inquiries can be directed to the corresponding author.

AUTHOR CONTRIBUTIONS

GQ provided the ideas and guided the entire experiment. WL and XG conducted experiments and data analysis and completed the manuscript. XG directed data analysis, manuscript writing and checking. XL and YZ contributed to the writing, translation and verification of the manuscript. All authors have read and agreed to the published version of the manuscript.

FUNDING

The study was supported by the National Key R and D Program of the Ministry of Science and Technology of China (grant No: 2018YFB1600100) and the National Natural Science Foundation of China (grant Nos: 51808058, and 52078065). This study was completed at the School of Traffic and Transportation Engineering, in Changsha University of Science and Technology.

REFERENCES

Allahverdi, A., Akhondi, M., and Mahinroosta, M. (2017). Superior Sodium Sulfate Resistance of a Chemically Activated Phosphorus Slag-Based Composite Cement. *J. Mater. Civil Eng.* 3. doi:10.1061/(asce)mt.1943-5533.0001762

Bujang, M., Hainin, M. R., Abd Majid, M. Z., Idham Mohd Satar, M. K., and Azahar, W. N. A. W. (2018). Assessment Framework for Pavement Material and Technology Elements in green Highway index. *J. Clean. Prod.* 174, 1240–1246. doi:10.1016/j.jclepro.2017.11.002

Colangelo, F., and Cioffi, R. (2013). Use of Cement Kiln Dust, Blast Furnace Slag and Marble Sludge in the Manufacture of Sustainable Artificial Aggregates by Means of Cold Bonding Pelletization. *Materials* 6, 3139–3159. doi:10.3390/ma6083139

Du, Q., Pan, T., Lv, J., Zhou, J., Ma, Q., and Sun, Q. (2019). Mechanical Properties of Sandstone Cement-Stabilized Macadam. *Appl. Sci.* 9, 3460. doi:10.3390/app9173460

Farhan, A. H., Dawson, A. R., and Thom, N. H. (2018). Damage Propagation Rate and Mechanical Properties of Recycled Steel Fiber-Reinforced and Cement-Bound Granular Materials Used in Pavement Structure. *Construction Building Mater.* 172, 112–124. doi:10.1016/j.conbuildmat.2018.03.239

Gao, Y. (2019). Theoretical Analysis of Reflective Cracking in Asphalt Pavement with Semi-rigid Base. *Iran J. Sci. Technol. Trans. Civ. Eng.* 43, 149–157. doi:10.1007/s40996-018-0154-8

Guo, J., Bao, Y., and Wang, M. (2018). Steel Slag in China: Treatment, Recycling, and Management. *Waste Manag.* 78, 318–330. doi:10.1016/j.wasman.2018.04.045

Hu, J. (2017). Comparison between the Effects of Superfine Steel Slag and Superfine Phosphorus Slag on the Long-Term Performances and Durability of concrete. *J. Therm. Anal. Calorim.* 128, 1251–1263. doi:10.1007/s10973-017-6107-9

Jing, H. J., Gou, M. J., and Song, L. C. (2021). Discrete Element Simulation of Bending Deformation of Geogrid-Reinforced Macadam Base. *Teh. Vjesn.* 28, 230–239. doi:10.17559/tv-20200623155019

JTG E42-2005 (2005). *Highway Engineering Aggregate Test Regulations*. Beijing: Research Institute of Highway Ministry of Transport.

JTG E51-2009 (2009). *Test Methods of Materials Stabilizing with Inorganic Binders for Highway Engineering*. Beijing: Research Institute of Highway Ministry of Transport.

Li, J., Shen, W., Zhang, B., Ji, X., Chen, X., Ma, W., et al. (2019). Investigation on the Preparation and Performance of Clinker-Fly Ash-gypsum Road Base Course Binder. *Construction Building Mater.* 212, 39–48. doi:10.1016/j.conbuildmat.2019.03.253

Li, S., Fan, M., Xu, L., Tian, W., Yu, H., and Xu, K. (2021). Rutting Performance of Semi-rigid Base Pavement in RIOHTrack and Laboratory Evaluation. *Front. Mater.* 7. doi:10.3389/fmats.2020.590604

Li, X. G., Xu, L. B., Dong, Y., Nie, X. P., and Shuai, S. X. (2015). Effect of Ultrafine Phosphorus Slag Addition on the Performance of Manufactured Sand Concrete with High Strength. *Rare Metal Mater. Eng.*, 365–368.

Lv, S., Peng, X., Yuan, J., Liu, H., Hu, L., Yang, S., et al. (2021a). Stress Path Investigation of Fatigue Characteristics of Cement Stabilized Macadam. *Construction Building Mater.* 292, 123446. doi:10.1016/j.conbuildmat.2021.123446

Lv, S., Xia, C., Liu, H., You, L., Qu, F., Zhong, W., et al. (2021b). Strength and Fatigue Performance for Cement-Treated Aggregate Base Materials. *Int. J. Pavement Eng.* 22, 690–699. doi:10.1080/10298436.2019.1634808

Lv, S., Xia, C., You, L., Wang, X., Li, J., and Zheng, J. (2019a). Unified Fatigue Characteristics Model for Cement-Stabilized Macadam under Various Loading Modes. *Construction Building Mater.* 223, 775–783. doi:10.1016/j.conbuildmat.2019.07.053

Ma, Y., Gu, J., Li, Y., and Li, Y. (2015). The Bending Fatigue Performance of Cement-Stabilized Aggregate Reinforced with Polypropylene Filament Fiber.

Construction Building Mater. 83, 230–236. doi:10.1016/j.conbuildmat.2015.02.073

Nanjegowda, V. H., and Biligiri, K. P. (2020). Recyclability of Rubber in Asphalt Roadway Systems: A Review of Applied Research and Advancement in Technology. *Resour. Conservation Recycling* 155, 104655. doi:10.1016/j.resconrec.2019.104655

Pang, M., Sun, Z., Chen, M., Lang, J., Dong, J., Tian, X., et al. (2020). Influence of Phosphorus Slag on Physical and Mechanical Properties of Cement Mortars. *Materials* 13, 2390. doi:10.3390/ma13102390

Piatak, N. M., Parsons, M. B., and Seal, R. R. (2015). Characteristics and Environmental Aspects of Slag: A Review. *Appl. Geochem.* 57, 236–266. doi:10.1016/j.apgeochem.2014.04.009

Qian, G., Bai, S., Ju, S., and Huang, T. (2013). Laboratory Evaluation on Recycling Waste Phosphorus Slag as the Mineral Filler in Hot-Mix Asphalt. *J. Mater. Civ. Eng.* 25, 846–850. doi:10.1061/(asce)mt.1943-5533.0000770

Qian, G. P., Yu, H. N., Gong, X. B., and Zheng, W. F. (2019). Effect of Phosphorus Slag Powder on Flammability Properties of Asphalt. *J. Mater. Civil Eng.* 11. doi:10.1061/(asce)mt.1943-5533.0002951

Shi, J., Tan, J., Liu, B., Chen, J., Dai, J., and He, Z. (2021). Experimental Study on Full-Volume Slag Alkali-Activated Mortars: Air-Cooled Blast Furnace Slag versus Machine-Made Sand as fine Aggregates. *J. Hazard. Mater.* 403, 123983. doi:10.1016/j.jhazmat.2020.123983

Sun, X., Liu, Z., Qin, X., Zeng, D., and Yin, Y. (2020a). Purifying Effect Evaluation of Pavement Surfacing Materials Modified by Novel Modifying Agent. *Front. Mater.* 7. doi:10.3389/fmats.2020.00180

Sun, X., Wu, S., Yang, J., and Yang, R. (2020b). Mechanical Properties and Crack Resistance of Crumb Rubber Modified Cement-Stabilized Macadam. *Construction Building Mater.* 259, 119708. doi:10.1016/j.conbuildmat.2020.119708

Tang, G., Liu, X., Zhou, L., Zhang, P., Deng, D., and Jiang, H. (2020). Steel Slag Waste Combined with Melamine Pyrophosphate as a Flame Retardant for Rigid Polyurethane Foams. *Adv. Powder Tech.* 31, 279–286. doi:10.1016/j.apt.2019.10.020

Vafaei, M., and Allahverdi, A. (2019). Strength Development and Acid Resistance of Geopolymer Based on Waste clay brick Powder and Phosphorous Slag. *Struct. Concrete* 20, 1596–1606. doi:10.1002/suco.201800138

Wang, Q., Zhuang, S., and Jia, R. (2019). An Investigation on the Anti-water Properties of Phosphorus Building gypsum (PBG)-based Mortar. *J. Therm. Anal. Calorim.* 136, 1575–1585. doi:10.1007/s10973-018-7825-3

Wang, Y., Xiao, R., Hu, W., Jiang, X., Zhang, X., and Huang, B. (2021). Effect of Granulated Phosphorus Slag on Physical, Mechanical and Microstructural Characteristics of Class F Fly Ash Based Geopolymer. *Construction Building Mater.* 291, 123287. doi:10.1016/j.conbuildmat.2021.123287

Xue, J., and Jiang, Y. (2017). Analysis on the Fatigue Properties of Vertical Vibration Compacted Lime-Fly Ash-Stabilized Macadam. *Construction Building Mater.* 155, 531–541. doi:10.1016/j.conbuildmat.2017.08.057

Yang, S., Li, P., Guo, M., Liao, S., and Wu, H. (2020). Study on Dynamic Load Monitoring of an Enhanced Stress Absorption Layer. *Front. Mater.* 7. doi:10.3389/fmats.2020.00148

You, L., Yue, Y., Yan, K., and Zhou, Y. (2020). Characteristics of Cement-Stabilized Macadam Containing Surface-Treated Recycled Aggregates. *Road Mater. Pavement Des.* 22, 2029–2043. doi:10.1080/14680629.2020.1740771

Zhang, J., and Cao, Y. (2012). Study on Leachate Treatment for Old Phosphorous Slag. *Desalination Water Treat.* 44, 75–82. doi:10.1080/19443994.2012.691779

Zheng, Y., Zhang, P., Cai, Y., Jin, Z., and Moshtagh, E. (2019). Cracking Resistance and Mechanical Properties of basalt Fibers Reinforced Cement-Stabilized Macadam. *Composites B: Eng.* 165, 312–334. doi:10.1016/j.compositesb.2018.11.115

Conflict of Interest: The authors declare that they have no known competing financial interests or personal relationships that could have appeared to influence the work reported in this article.

Publisher's Note: All claims expressed in this article are solely those of the authors and do not necessarily represent those of their affiliated organizations, or those of the publisher, the editors and the reviewers. Any product that may be evaluated in this article, or claim that may be made by its manufacturer, is not guaranteed or endorsed by the publisher.